

Water-Mediated Carbon-Oxygen Hydrogen Bonding Facilitates AdoMet Recognition in the Reactivation Domain of Cobalamin-dependent Methionine Synthase

Robert J. Fick, Mary C Clay, Lucas Vander Lee, Steve Scheiner, Hashim M. Al-Hashimi, and Raymond C. Trievle

Biochemistry, Just Accepted Manuscript • DOI: 10.1021/acs.biochem.8b00375 • Publication Date (Web): 07 May 2018

Downloaded from <http://pubs.acs.org> on May 8, 2018

Just Accepted

"Just Accepted" manuscripts have been peer-reviewed and accepted for publication. They are posted online prior to technical editing, formatting for publication and author proofing. The American Chemical Society provides "Just Accepted" as a service to the research community to expedite the dissemination of scientific material as soon as possible after acceptance. "Just Accepted" manuscripts appear in full in PDF format accompanied by an HTML abstract. "Just Accepted" manuscripts have been fully peer reviewed, but should not be considered the official version of record. They are citable by the Digital Object Identifier (DOI®). "Just Accepted" is an optional service offered to authors. Therefore, the "Just Accepted" Web site may not include all articles that will be published in the journal. After a manuscript is technically edited and formatted, it will be removed from the "Just Accepted" Web site and published as an ASAP article. Note that technical editing may introduce minor changes to the manuscript text and/or graphics which could affect content, and all legal disclaimers and ethical guidelines that apply to the journal pertain. ACS cannot be held responsible for errors or consequences arising from the use of information contained in these "Just Accepted" manuscripts.



ACS Publications

is published by the American Chemical Society, 1155 Sixteenth Street N.W., Washington, DC 20036

Published by American Chemical Society. Copyright © American Chemical Society. However, no copyright claim is made to original U.S. Government works, or works produced by employees of any Commonwealth realm Crown government in the course of their duties.

1
2
3 **Water-Mediated Carbon-Oxygen Hydrogen Bonding Facilitates AdoMet Recognition in**
4 **the Reactivation Domain of Cobalamin-dependent Methionine Synthase**
5
6
7
8
9
10
11

12 Robert J. Fick¹, Mary C. Clay², Lucas Vander Lee¹, Steve Scheiner³, Hashim Al-Hashimi², and
13 Raymond C. Trievel^{1*}
14
15

16
17 ¹Department of Biological Chemistry, University of Michigan, Ann Arbor, MI 48109, USA
18
19

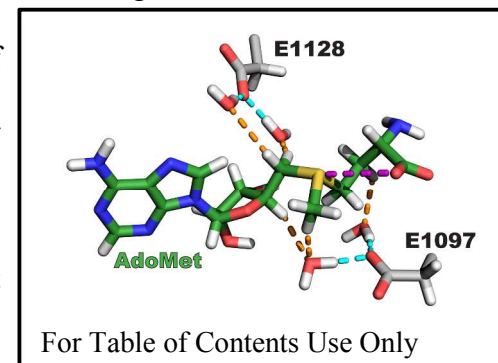
20 ²Department of Biochemistry, Duke University, Durham, NC 27710, USA
21
22

23 ³Department of Chemistry and Biochemistry, Utah State University, Logan, UT 84322, USA
24
25
26
27
28
29
30
31

32 *Corresponding Author: Raymond Trievel
33
34 Address: University of Michigan
35
36 Department of Biological Chemistry
37
38 1150 West Medical Center Drive
39
40 5301 Medical Science Research Building III
41
42 Ann Arbor, MI 48109
43
44
45 E-mail: rtrievel@umich.edu
46
47
48 Phone: 734-647-0889
49
50 FAX: 734-763-4581
51
52
53
54
55
56
57
58
59
60

Abstract

The C-terminal domain of cobalamin-dependent methionine synthase (MetH) has an essential role in catalyzing the reactivation of the enzyme following the oxidation of its cobalamin cofactor. This reactivation occurs through reductive methylation of the cobalamin using S-adenosylmethionine (AdoMet) as the methyl donor. Herein, we examine the molecular recognition of AdoMet by the MetH reactivation domain utilizing structural, biochemical, and computational approaches. Crystal structures of the *E. coli* MetH reactivation domain in complex with AdoMet, the methyl transfer product S-adenosylhomocysteine (AdoHcy), and the AdoMet analog inhibitor sinefungin illustrate that the ligands exhibit an analogous conformation within the solvent-exposed substrate binding cleft of the enzyme. AdoMet binding is stabilized by an intramolecular sulfur-oxygen chalcogen bond between the sulfonium and carboxylate groups of the substrate and by water-mediated carbon-oxygen hydrogen bonding between the sulfonium cation and the side chains of Glu1097 and Glu1128 that bracket the substrate binding cleft. AdoMet and sinefungin exhibited similar binding affinities for the MetH reactivation domain, whereas AdoHcy displayed an affinity for the enzyme that was an order of magnitude lower. Mutations of Glu1097 and Glu1128 diminished the AdoMet/AdoHcy binding selectivity ratio to approximately twofold, underscoring the role of these residues in enabling the enzyme to discriminate between substrate and product. Together, these findings indicate that Glu1097 and Glu1128 in MetH promote high affinity recognition of AdoMet and that sinefungin and potentially other AdoMet-based methyltransferase inhibitors can abrogate MetH reactivation, which would result in off-target effects associated with alterations in methionine



1
2
3 homeostasis and one-carbon metabolism.
4
5

6 INTRODUCTION

7

8 Cobalamin-dependent methionine synthase (MetH) is a dynamic multi-domain enzyme
9 that has a central role in one carbon metabolism by catalyzing the methylation of homocysteine
10 to methionine using methyltetrahydrofolate ($\text{CH}_3\text{-H}_4\text{folate}$). In MetH, this reaction occurs
11 through the transfer of a methyl group from $\text{CH}_3\text{-H}_4\text{folate}$ to cob(I)alamin (Co(I)Cbl) to form
12 $\text{CH}_3\text{-Co(III)Cbl}$, which subsequently methylates homocysteine to yield methionine.¹⁻³ During
13 turnover under aerobic conditions, Co(I)Cbl is oxidized to Co(II)Cbl every $\sim 2,000$ reactions,
14 inactivating the enzyme.⁴ MetH activity is restored through a one electron reduction of Co(II)Cbl
15 to Co(I)Cbl by MetH reductase, coupled with S-adenosylmethionine (AdoMet)-dependent
16 methylation of the coenzyme by the C-terminal reactivation domain of MetH. The methionine
17 generated by MetH is utilized in protein synthesis and the biosynthesis of AdoMet, the
18 predominant methyl donor utilized in metabolic pathways, cellular signaling, and gene
19 regulation. Thus, the reactivation domain of MetH plays an essential role in maintaining methyl
20 homeostasis in biological systems.
21
22

23 Biochemical and structural studies have provided important insights into the mechanism
24 of reactivation of MetH by its C-terminal domain. Initial structural characterization of the *E. coli*
25 MetH reactivation domain by Dixon *et al.* revealed that it adopts a crescent-shaped fold that is
26 unique from other classes of AdoMet-dependent methyltransferases, leading to its categorization
27 as a Class II methyltransferase.^{5, 6} AdoMet binds in a relatively solvent-exposed cleft in the
28 concave face of the domain. Two glutamate residues, Glu1097 and Glu1128, flank the AdoMet
29 binding site but do not directly interact with the substrate. However, the proximity of these
30 glutamates to AdoMet was proposed to promote substrate recognition through electrostatic
31 interactions.
32
33

1
2
3 interactions with the substrate's sulfonium cation. Subsequent structural and functional studies of
4 MetH have demonstrated that the exposed AdoMet binding cleft in the reactivation domain
5 permits the substrate to dock with the large planar corrin ring system in the cobalamin binding
6 domain, facilitating methylation of the cofactor during enzyme reactivation.⁷⁻⁹
7
8
9
10
11

12 A recent survey of representative high resolution crystal structures from several classes of
13 AdoMet-dependent methyltransferases has revealed the widespread presence of carbon-oxygen
14 (CH \cdots O) hydrogen bonds between the AdoMet methyl group and oxygen atoms with the
15 enzymes' active sites.¹⁰ These interactions have been shown to be important in high affinity
16 AdoMet recognition and for promoting catalysis in the SET domain class of lysine
17 methyltransferases. Interestingly, the structure of the MetH reactivation domain bound to
18 AdoMet does not exhibit direct CH \cdots O hydrogen bonding between the AdoMet methyl group
19 and the enzyme, in contrast to other classes of methyltransferases. This observation spurred us to
20 examine whether other interactions with the active site are important in conferring substrate
21 specificity in MetH.
22
23
24
25
26
27
28
29
30
31
32
33
34
35
36
37

EXPERIMENTAL PROCEDURES

40 **Reagents.** S-adenosylhomocysteine and sinefungin were purchased from Millipore-Sigma. S-
41 adenosylmethionine p-toluenesulfonate was purchased from Carbosynth and purified by ion-
42 exchange chromatography.¹¹ $^{13}\text{CH}_3$ -AdoMet was enzymatically synthesized using *E. coli*
43 AdoMet synthetase with methyl- ^{13}C methionine (Cambridge Isotope Laboratories) and
44 adenosine triphosphate, and purified as previously described.¹¹
45
46
47
48
49
50
51
52
53

54 **Protein Expression and Purification.** The cDNA encoding the C-terminal domain of *E. coli*
55
56
57
58
59
60

1
2
3 MetH (residues 897 – 1227; UniProt Accession ID P13009) was cloned into a variant of pET15b
4 with a tobacco etch virus (TEV) protease-cleavable N-terminal hexahistidine tag. The E1097Q
5 and E1128Q mutations were prepared using QuikChange mutagenesis (Agilent) and were
6 confirmed using dideoxy sequencing. Expression vectors were transformed into *E. coli* Rosetta2
7 DE3 cells (Novagen) cultured in 2xYT media, and protein expression was induced at 18 °C
8 overnight. The WT MetH reactivation domain and glutamine mutants were purified using a
9 combination of Co(II) Talon affinity and Superdex 200 gel filtration chromatography (GE
10 Healthcare). Prior to gel filtration purification, the protein was incubated with charcoal to
11 remove AdoMet that co-purified with the enzyme, as previously described.¹² The purified
12 proteins were concentrated, flash frozen in liquid nitrogen, and stored at -80 °C. Protein
13 concentrations were determined by their absorbance at 280 nm.
14
15
16
17
18
19
20
21
22
23
24
25
26
27
28
29
30

31 **Crystallization and Structure Determination.** The MetH reactivation domain was crystallized
32 using the hanging drop method in 60 – 100 mM TRIS pH 7.2 - 7.5, 300 mM magnesium acetate
33 and 27 - 32% PEG 6000, similar to the previously reported crystallization conditions.⁵ The
34 protein solution contained 15mg/mL MetH, 10 mM TRIS pH 7.4, 10 mM EDTA, and 3.0 mM
35 AdoMet, 3.0 mM sinefungin, or 5.0 mM AdoHcy. X-ray diffraction data were collected at the
36 Life Sciences Collaborative Access Team beamline 21-ID-G at the Advanced Photon Source
37 Synchrotron, Argonne National Laboratory and were processed using HKL2000.¹³ Structures of
38 the MetH complexes were determined by molecular replacement using Phaser with the
39 coordinates of the *E. coli* MetH reactivation domain (PDB: 1MSK) as the search model.¹⁴ Model
40 building, refinement, and validation were performed using Coot and Phenix.¹⁵⁻¹⁷ Structural
41
42
43
44
45
46
47
48
49
50
51
52
53
54
55
56
57
58
59
60

1
2
3 figures were rendered using PyMOL (Schrödinger, LLC), and electrostatic surface calculations
4 were performed using the APBS plugin for PyMOL.¹⁸
5
6
7
8
9

10 **Isothermal Titration Calorimetry.** ITC was performed using a MicroCal VP-ITC calorimeter
11 (Malvern Instruments) for WT MetH and a MicroCal Auto-iTC200 (Malvern Instruments) for
12 the MetH E1097Q and E1128Q mutants. Titrations were performed using 20 mM sodium
13 phosphate pH 8.0 and 100 mM sodium chloride. Experiments with the WT enzyme and AdoMet
14 or sinefungin were performed with 60 μ M protein and 600 μ M ligand, whereas the AdoHcy
15 titrations were carried out with 200 μ M protein and 2.2 mM ligand. Experiments using the
16 E1097Q and E1128Q mutants utilized 830 – 940 μ M protein and 9.6 mM AdoMet, 16.1 mM
17 sinefungin, or 10.1 – 10.7 mM AdoHcy. The sinefungin titrations with the MetH mutants
18 required a higher concentration of ligand. Control titrations of sinefungin at these higher
19 concentrations, which approached the concentration of the phosphate buffer, exhibited a
20 significant background heat, potentially due to titration of the amine group in sinefungin. To
21 correct for this effect, sinefungin was dissolved in buffer and the solution was adjusted to pH 8.0
22 using 200 mM HCl in a 20 mM sodium phosphate and 100 mM sodium chloride (final
23 concentration) to maintain the phosphate and sodium ion concentrations. Data were processed
24 using Origin (OriginLab Corp.). Stoichiometries of binding (N values) ranged from 0.9 to 1.1.
25
26
27
28
29
30
31
32
33
34
35
36
37
38
39
40
41
42
43
44
45
46
47
48
49
50
51
52
53
54
55
56
57
58
59
60

NMR Spectroscopy. All NMR experiments were performed on a Bruker Avance III 600 MHz
spectrometer equipped with a 5-mm triple-resonance cryogenic probe. Spectra were recorded at
25 °C using 0.2 mM ¹³CH3-AdoMet in 20 mM sodium phosphate, 100 mM NaCl, and 10% D₂O
at pH 7.0 (SET7/9) or pH 8.0 (MetH), and referenced relative to the water signal. Data were

1
2
3 processed and analyzed using NMRPipe and Sparky, respectively.^{19, 20} The enzyme-bound
4 chemical shift was determined using ¹H-¹³C Heteronuclear Single Quantum Correlation (HSQC)
5 spectra of ¹³C-methyl labeled AdoMet were recorded in the presence and absence of a 1.2 molar
6 stoichiometric excess of SET7/9 or MetH (0.24 mM). ¹H-¹³C Band-Selective Optimized Flip
7 Angle Short Transient Heteronuclear Multiple Quantum Correlation (SOFAST-HMQC) spectra
8 were also recorded to assess the relative solvent accessibility of the enzyme-bound AdoMet.
9
10
11
12
13
14
15
16
17
18

19 **QM Calculations.** All quantum calculations were carried out within the framework of the
20 Gaussian-09 set of codes.²¹ The 6-31+G** basis set was applied at the DFT level, using the
21 M06-2X functional.²² Geometries were fully optimized under the restriction that certain atoms
22 were held in their crystallographic coordinates. Optimizations were carried out in aqueous
23 solvent, using the CPCM variant²³ of self-consistent reaction field theory. The binding energy,
24 E_B , of each complex was evaluated in vacuo as the difference between the energy of the entire
25 complex and the sum of the energies of a) the $\text{MeS}^+(\text{Et})_2$ and $\text{S}(\text{Et})_2$ monomers, representing
26 AdoMet and AdoHcy and b) the propionate and propionamide group and their cognate water
27 molecules, mimicking Glu1097 and Glu1128 and their corresponding glutamine mutations with
28 the water molecules bridging to the ligands.
29
30
31
32
33
34
35
36
37
38
39
40
41
42
43
44

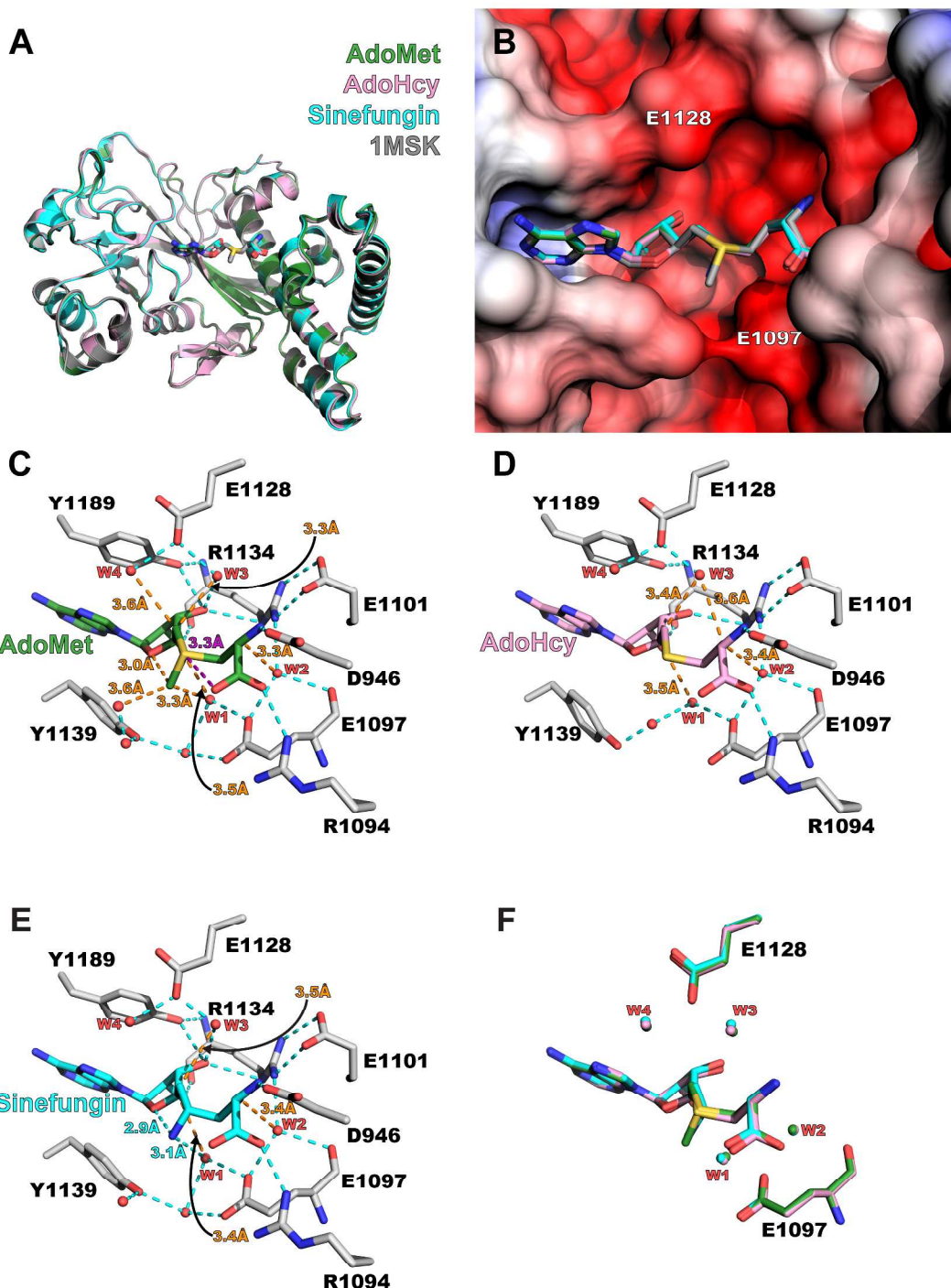
RESULTS

45
46
47 To gain molecular insights into its substrate specificity, we determined high resolution
48 crystal structures of the *E. coli* MetH reactivation domain bound to AdoMet, AdoHcy, and the
49 AdoMet analog inhibitor sinefungin (Table S1). The modeling of the ligands in the structures
50 was verified using simulated annealing omit maps (Figure S1). Superimposition of the
51
52
53
54
55
56
57
58
59
60

1
2
3 reactivation domain complexes and the previously reported structure of the MetH•AdoMet
4 complex illustrates their high degree of structural similarity, with root mean squared deviations
5 for the aligned C α atoms of ≤ 0.32 Å (Figure 1A). Further, the structural alignment of the
6 complexes reveals that AdoMet, AdoHcy, and sinefungin adopt nearly identical conformations
7 when bound in the enzyme's solvent-exposed substrate binding cleft (Figure 1B). This
8 conformation is distinct from the AdoMet binding modes observed in other classes of
9 methyltransferases and is stabilized in part by an intramolecular S \cdots O chalcogen bond between
10 carboxylate and sulfonium ions in the substrate (Figure 1C), analogous to the chalcogen bond
11 formed by AdoMet and an asparagine in the lysine methyltransferase SET7/9.¹² Further, the
12 AdoMet methyl group and the ether O4 atom in the ribose ring are oriented in a geometry
13 consistent with an intramolecular CH \cdots O hydrogen bond. In addition to these intramolecular
14 interactions, an extensive network of direct and water-mediated hydrogen bonds and van der
15 Waals interactions between AdoMet and the residues composing the binding pocket in the
16 enzyme facilitate substrate recognition. An examination of the AdoHcy and sinefungin
17 complexes reveals an analogous network of intermolecular interactions that promote binding of
18 the enzyme to the product and inhibitor, respectively (Figure 1D and 1E). Correlatively,
19 superimposition of the three MetH complexes illustrates an analogous conformation adopted by
20 AdoMet, AdoHcy, and sinefungin (Figure 1F).
21
22
23
24
25
26
27
28
29
30
31
32
33
34
35
36
37
38
39
40
41
42
43
44
45
46
47

48 **Figure 1.** Crystal structures of the MetH complexes. (A) Superimposition of the MetH
49 complexes of AdoMet (green), AdoHcy (pink), sinefungin (cyan), and the previously determined
50 MetH•AdoMet complex (PDB: 1MSK; gray). (B) Electrostatic surface of the substrate binding
51 cleft with AdoMet, sinefungin, and AdoHcy aligned based on the superimposition from panel A.
52 The electrostatic potential is contoured from -5.0 to 5.0 kT/e with red and blue denoting acidic
53 and basic surfaces, respectively. The positions of Glu1097 and 1128 and labeled, and the ligands
54 are colored according to the scheme used in panel A. Structures of the MetH substrate binding
55 are colored according to the scheme used in panel A. Structures of the MetH substrate binding
56

1
2
3 cleft bound to AdoMet (C), AdoHcy (D), and sinefungin (E). Conventional hydrogen bonds are
4 depicted by cyan dashes, whereas CH \cdots O hydrogen bonds are denoted as orange dashes.
5 Distances for the hydrogen bonds formed by the four water molecules (W1 – W4) that mediate
6 interactions between the ligands and Glu1097 and Glu1128 are illustrated. (F) Structural overlay
7 of ligands, Glu1097, Glu1128, and the four water molecules in the AdoMet, AdoHcy, and
8 sinefungin complexes from the superimposition in panel A. The water molecules and glutamate
9 side chains are colored according to their corresponding ligand.
10
11
12
13
14
15
16
17
18
19
20
21
22
23
24
25
26
27
28
29
30
31
32
33
34
35
36
37
38
39
40
41
42
43
44
45
46
47
48
49
50
51
52
53
54
55
56
57
58
59
60



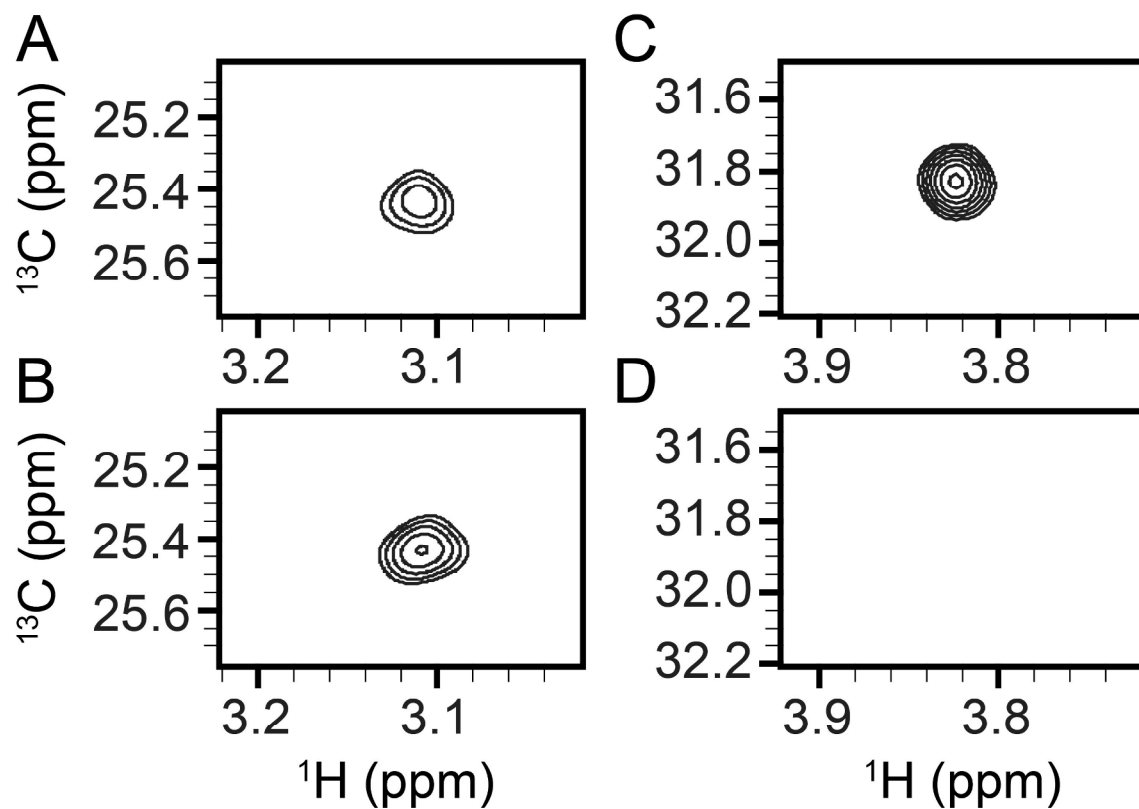
Given the similarity in the ligands' binding modes and their interactions with MetH reactivation domain, we sought to understand the determinants that confer selectivity in AdoMet recognition. Initial structural studies of the reactivation domain by Dixon *et al.* suggested Glu1097 and Glu1128 as being important to AdoMet binding (Figure 1C).⁵ The side chains of these residues are located within 6 Å of the sulfur cation of the substrate but do not participate in direct interactions with sulfonium group. They proposed that electrostatic interaction between the carboxylate groups of Glu1097 and Glu1128 and the AdoMet sulfonium cation would favor binding of the substrate compared to the product AdoHcy in which the sulfonium is replaced by a neutral thioether moiety. Consistent with this observation, electrostatic surface calculations of the MetH reactivation domain illustrate that the substrate binding cleft is relatively acidic, conducive to the recognition of the AdoMet sulfonium cation (Figure 1B).

A close inspection of the substrate binding cleft reveals two pairs of water molecules that mediate hydrogen bonding between AdoMet and Glu1097 and Glu1128. For clarity, we have termed these water molecules W1, W2, W3, and W4. W1 facilitates CH \cdots O hydrogen bonding between the Glu1097 carboxylate group and the AdoMet methyl group and the C4 atom in the ribose ring, whereas W2 serves to bridge hydrogen bonding between Glu1097 and the C β methylene group of the substrate (Figure 1C). The C β and C4 atoms in AdoMet are one carbon atom removed from the sulfur cation but remain partially polarized due to their proximity to the cation and can participate in CH \cdots O hydrogen bonding, albeit more weakly than a carbon atom bonded directly to the sulfur cation.²⁴ W3 and W4 form a CH \cdots O hydrogen bonding bridge between the Glu1128 carboxylate anion and the C5 methylene group in the substrate. In addition, W3 forms an OH \cdots O hydrogen bond to the 3'-hydroxyl group of the ribose ring of AdoMet. A superimposition of the structures of the AdoMet, AdoHcy, and sinefungin complexes illustrates

1
2
3 that the four water molecules occupy analogous positions within the substrate binding cleft of the
4 different ligand-bound complexes (Figure 1F). Collectively, the structures illustrate that AdoMet,
5 AdoHcy, and sinefungin adopt nearly identical conformations when bound to the MetH
6 reactivation domain and that water molecules serve to bridge the interactions between the
7 AdoMet sulfonium cation and Glu1097 and Glu1128 within the enzyme's binding cleft.
8
9

10
11
12
13
14 Based upon our observations in the MetH crystal structures, we sought to further examine
15 the water-mediated CH \cdots O hydrogen bonding between MetH and the AdoMet methyl group in
16 solution. In prior studies with the lysine methyltransferase SET7/9, we employed two-
17 dimensional heteronuclear single quantum coherence (2D HSQC) spectroscopy with a [^{13}C]-
18 labeled methyl group of AdoMet ($^{13}\text{CH}_3$ -AdoMet) to detect CH \cdots O hydrogen bonding between
19 the substrate's methyl group and residues within the enzyme's active site. In the 2D-HSQC
20 spectrum of the MetH- $^{13}\text{CH}_3$ -AdoMet complex, the ^1H chemical shift of the methyl group was
21 observed at 3.1 ppm, a 0.1 ppm downfield change compared to the reported value of AdoMet
22 free in solution (3.0 ppm) (Figure 2A).²⁵ This small alteration in the ^1H chemical shift is
23 consistent with the water-mediated CH \cdots O hydrogen bonding of the AdoMet methyl group
24 bound to MetH (Figure 2A). In contrast, the ^1H chemical shift of $^{13}\text{CH}_3$ -AdoMet bound to the
25 lysine methyltransferase SET7/9 exhibited a marked downfield change of 3.8 ppm (Figure 2B),
26 consistent with methyl CH \cdots O hydrogen bonding in the active site, as previously reported.¹¹
27
28 Corroborating these findings, a cross-peak was recorded in the band-selective optimized flip
29 angle short transient heteronuclear multiple quantum coherence (SOFAST HMQC)²⁶ spectrum of
30 the MetH- $^{13}\text{CH}_3$ -AdoMet complex, whereas no peak was discernable in the spectrum of the
31 SET7/9- $^{13}\text{CH}_3$ -AdoMet complex (Figure 2C & 2D). The SOFAST HMQC data concur with the
32 relatively solvent-exposed proton rich environment of the AdoMet binding cleft in MetH and the
33
34
35
36
37
38
39
40
41
42
43
44
45
46
47
48
49
50
51
52
53
54
55
56
57
58
59
60

1
2
3 general depletion of the ^1H - ^1H “relaxation sink” around the substrate’s methyl group when
4 bound in the active site of SET7/9 (Figure S2). Together, the NMR results correlate with the
5 MetH crystal structures, illustrating the relative solvent exposure AdoMet methyl group when
6 bound in the active site.
7
8
9
10
11
12
13
14
15
16



48
49 **Figure 2.** Two-dimensional HSQC (A) and SOFAST-HMQC (B) of the MetH- $^{13}\text{CH}_3$ -AdoMet
50 complex, and HSQC (C) and SOFAST-HMQC (D) of the SET7/9- $^{13}\text{CH}_3$ -AdoMet complex.
51
52
53
54
55
56
57
58
59
60

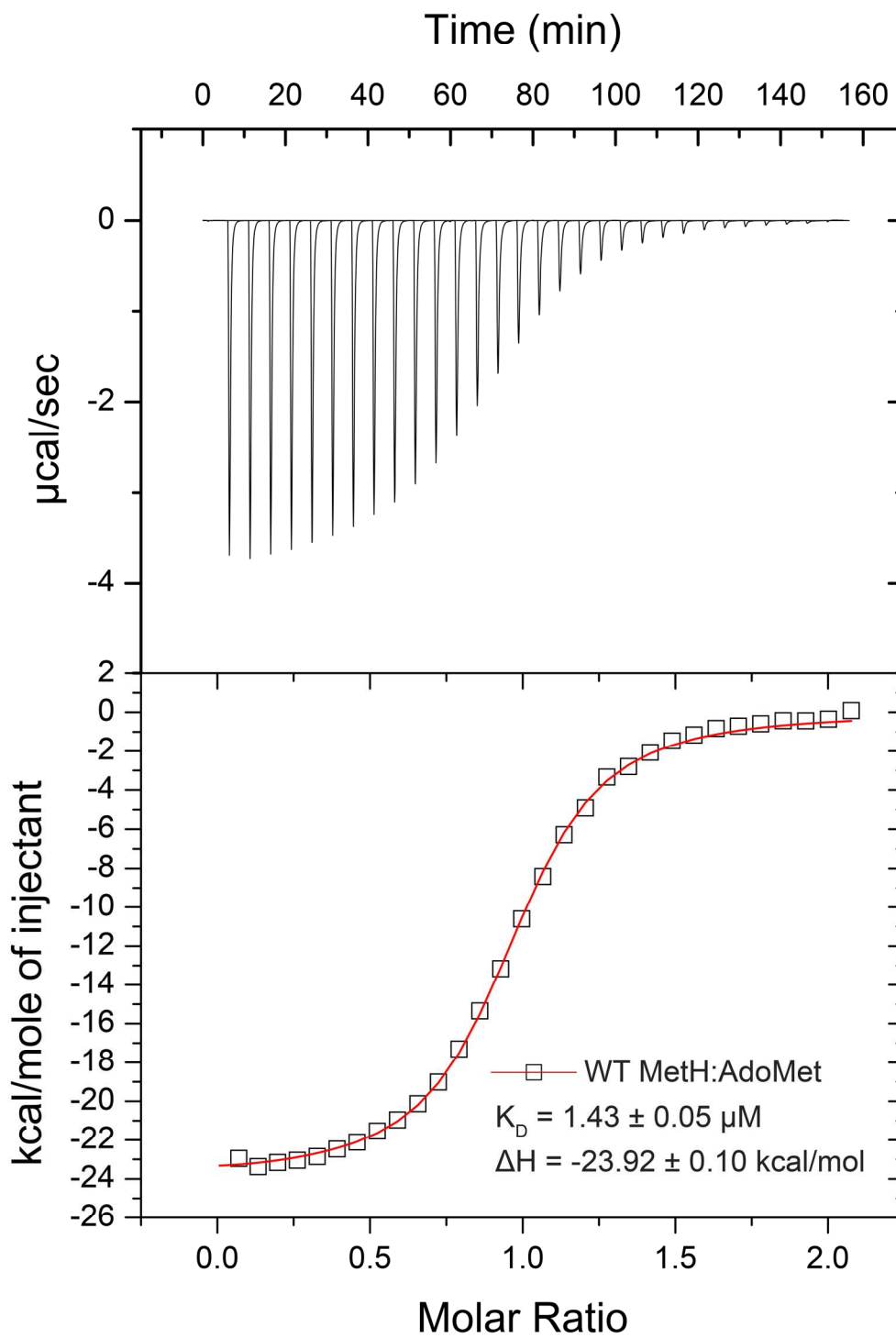
1
2
3 Our observations of water-mediated CH \cdots O hydrogen bonding between Glu1097 and
4 Glu1128 in MetH and the AdoMet sulfonium cation prompted us to examine the thermodynamic
5 properties of these interactions and whether they contribute toward the substrate specificity of
6 the enzyme. Using isothermal titration calorimetry (ITC), we measured the equilibrium
7 dissociation constants (K_D) and enthalpies of binding (ΔH) of AdoMet, AdoHcy, and sinefungin
8 for the wild type (WT) enzyme (Figure 3 and Figure S3A and S3B). The ITC data illustrate that
9 the MetH reactivation domain bound AdoMet and sinefungin with comparable affinity and ΔH
10 values, whereas it exhibited a 15-fold lower affinity for AdoHcy compared to AdoMet, with a
11 corresponding decrease in ΔH (Table 1). These results are consistent with the acidic surface of
12 the substrate binding cleft and the water-mediated hydrogen bonding between the carboxylate
13 anions of Glu1097 and Glu1128 and the sulfonium and ammonium cations of AdoMet and
14 sinefungin, respectively (Figure 1B, 1C, and 1D). These water-mediated hydrogen bonds would
15 presumably be relatively strong due to the positive and negative charges of the proton donors and
16 acceptors, respectively. Conversely, AdoHcy would presumably be expected to form weaker
17 water-mediated CH \cdots O hydrogen bonds with the glutamates due to the lack of methyl
18 interactions and its neutral thioester group, consistent with the thermodynamic binding data. To
19 further probe these findings, we substituted Glu1097 and Glu1128 by glutamine in MetH and
20 examined the effect of these mutations on the binding affinity of the ligands (Figure S3C – S3H).
21 Glutamine mutations were chosen due to their propensity to weaken the water-mediated
22 hydrogen bonding to the ligands by substituting their side chain carboxylate anions with neutral
23 carboxamide groups, while preserving the hydrogen bonding networks formed by these residues
24 within the active site (Figure S4). The E1097Q and E1128Q mutations diminished the binding
25 affinity of AdoMet and sinefungin from 4- to 22-fold compared to WT MetH, whereas binding to
26
27
28
29
30
31
32
33
34
35
36
37
38
39
40
41
42
43
44
45
46
47
48
49
50
51
52
53
54
55
56
57
58
59
60

AdoHcy was altered by less than two-fold. Moreover, each glutamine mutation effectively reduced the difference in the enzyme's binding selectively for AdoMet and AdoHcy to approximately two-fold. Together, these findings illustrate that the water-mediated CH \cdots O hydrogen bonds formed between the carboxylate groups of Glu1097 and Glu1128 and the AdoMet sulfonium cation are important in conferring recognition of the substrate versus the product and that glutamine substitutions of these residues abrogates this selectively.

Table 1. ITC data and QM calculated binding energies (E_B) for ligand binding by WT MetH and the E1097Q and E1128Q mutants.

	K_D (μM)					
	WT	E1097Q	E1128Q			
AdoMet	1.43 \pm 0.05	6.10 \pm 0.68	17.5 \pm 1.0			
AdoHcy	20.8 \pm 0.2	15.0 \pm 0.5	38.2 \pm 1.0			
Sinefungin	2.04 \pm 0.07	17.7 \pm 1.56	44.8 \pm 2.51			
	ΔH (kcal mol $^{-1}$)					
	WT	E1097Q	E1128Q			
AdoMet	-23.92 \pm 0.10	-19.43 \pm 0.16	-15.65 \pm 0.09			
AdoHcy	-15.30 \pm 0.03	-11.95 \pm 0.04	-11.22 \pm 0.04			
Sinefungin	-18.59 \pm 0.09	-17.02 \pm 0.17	-14.63 \pm 0.13			
	QM binding energies (kcal mol $^{-1}$)					
	E1097	Q1097	ΔE_B [E-Q]	E1128	Q1128	ΔE_B [E-Q]
MeS $^+$ (Et) $_2$ complex energy	87.69	19.19	68.50	73.41	29.30	44.11
S(Et) $_2$ complex energy	8.45	7.25	1.20	6.30	3.53	2.77
ΔE_B [MeS $^+$ (Et) $_2$ - S(Et) $_2$]	79.24	11.94		67.11	25.77	

Figure 3. ITC titration of the WT MetH reactivation domain and AdoMet. The upper panel shows the titration of AdoMet into the MetH solution, and the lower panel illustrates the curve fitted to the binding isotherm.



1
2
3 To further investigate these findings, we performed quantum mechanical calculations to
4 investigate the CH \cdots O hydrogen bonding between AdoMet and AdoHcy and the glutamates
5 within the MetH substrate binding cleft. To assess the individual contributions of Glu1097 and
6 Glu1128 to AdoMet and AdoHcy recognition, pairwise models of the active site were generated
7 comprising the ligands, each glutamate, and the cognate water molecules that mediate CH \cdots O
8 hydrogen bonding. The active site models were based upon the coordinates of the crystal
9 structures of MetH bound to the substrate and product (Figure 4 and Figure S5). The AdoMet
10 sulfonium cation and AdoHcy thioester were represented as $\text{MeS}^+(\text{Et})_2$ and $\text{S}(\text{Et})_2$ monomers, as
11 previously described.^{12, 27} Glu1097 and Glu1128 were modeled as propionate groups, and the
12 corresponding glutamine substitutions were represented as propionamide moieties using the
13 coordinates of the glutamate side chains, with the carboxamide oxygen atoms oriented toward
14 the ligands to retain an analogous pattern of water-mediated CH \cdots O hydrogen bonding. For the
15 models representing the WT enzyme, the heavy atoms of the ligands and the water molecules
16 were constrained to their crystallographic coordinates, whereas certain carbon atoms in the
17 propionate were constrained to maintain the glutamate side chain conformations observed in the
18 crystal structures. For the propionamide-containing models, the same atoms were held fixed in
19 the ligands and propionamide groups. However, the water molecules were left unrestrained to
20 allow the optimization of their positions relative to the propionamide monomers, with the
21 exception of W4 in the $\text{S}(\text{Et})_2$ model that strayed into a position that would sterically clash with
22 atoms in the crystal structures that were not included in the models.
23
24
25
26
27
28
29
30
31
32
33
34
35
36
37
38
39
40
41
42
43
44
45
46
47
48
49
50
51
52
53
54
55
56
57
58
59
60

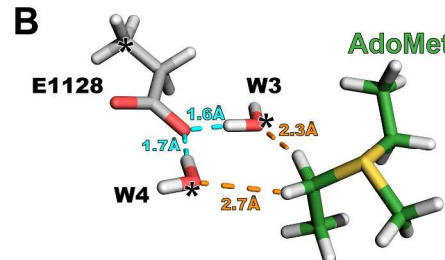
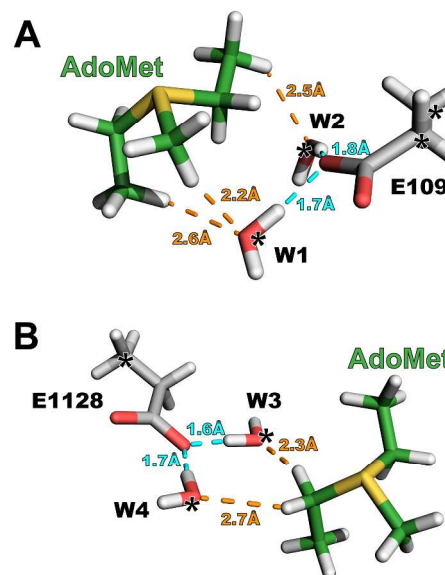


Figure 4. Optimized geometry for the minimal active site models used in the QM calculations to determine the binding energies for the AdoMet and Glu1097 (A) and AdoMet and Glu1128 complexes (B). The AdoMet sulfonium cation was modeled as $\text{MeS}^+(\text{Et})_2$, and the glutamate side chains were represented by propionate groups. The ligand heavy atom positions (carbon and sulfur atoms) were constrained to their X-ray coordinates, as were the oxygen atoms in the water molecules and carbon atoms in the propionate monomers that are denoted by asterisks. Conventional and $\text{CH}\cdots\text{O}$ hydrogen bonds are depicted by cyan and orange dashed lines, respectively with $\text{H}\cdots\text{O}$ distances denoted.

Once the active site models were generated, the binding energy (E_B) for each complex was evaluated as the energy difference between the full complex on one hand and the sum of the ligand and the interacting residue and solvent on the other. We then computed the differences in the E_B values for the $\text{MeS}^+(\text{Et})_2$ and $\text{S}(\text{Et})_2$ complexes ($\Delta E_B [\text{MeS}^+(\text{Et})_2 - \text{S}(\text{Et})_2]$) and the propionate to propionamide substitutions corresponding to the E1097Q and E1128Q mutations ($\Delta E_B [\text{E} - \text{Q}]$) (Table 1). Overall, the trends observed in the E_B values for the models correlate with the AdoMet and AdoHcy binding affinities and ΔH values observed for the WT MetH and the E1097Q and E1128Q mutants. There is a substantial decrease in the $\Delta E_B [\text{MeS}^+(\text{Et})_2 - \text{S}(\text{Et})_2]$ values upon substitution of the propionate group by propionamide for both the Glu1097 and Glu1128 models. This finding is consistent with the ITC data illustrating that the differences in the binding affinities for AdoMet and AdoHcy are substantially diminished in the E1097Q and E1128Q mutations compared to the WT MetH. Correlatively, the values of $\Delta E_B [\text{E} - \text{Q}]$ are substantially larger for the $\text{MeS}^+(\text{Et})_2$ models compared to $\text{S}(\text{Et})_2$ models for both glutamate positions, in agreement with the greater apparent effect of the E1097Q and E1128Q mutants on the binding affinities and ΔH values for AdoMet relative to AdoHcy. Taken together, the strongest binding energies are observed when both the sulfonium cation and carboxylate anions are present in the models, whereas the interaction energies are diminished with the substitution of neutral thioether or carboxamide groups, respectively. These results indicate that the water-mediated hydrogen bonding serves as a conduit for the electrostatic interactions between the AdoMet sulfonium cation and the Glu1097 and Glu1128 carboxylate anions and that the strength of these interactions is significantly attenuated when one or both ions is substituted by a neutral moiety.

DISCUSSION

Prior studies of different classes of AdoMet-dependent methyltransferases have described the presence of $\text{CH}\cdots\text{O}$ hydrogen bonding between the AdoMet sulfonium cation and residues within the enzymes' active sites.¹⁰ In SET domain lysine methyltransferases, these interactions have been shown to be important for high affinity recognition of AdoMet, enabling these enzymes to distinguish the substrate from the product AdoHcy, thus mitigating product inhibition.^{10, 27, 28} In contrast, the substrate binding cleft of MetH utilizes a different mode of recognition wherein active site glutamates form water mediated $\text{CH}\cdots\text{O}$ hydrogen bonds with AdoMet sulfonium cation. The electrostatic nature of these hydrogen bonds is important, as the removal of one or both charges by glutamate to glutamine mutation or substitution of the AdoMet sulfonium cation by the thioether in AdoHcy diminished the binding affinity, ΔH values, and the QM calculated E_B values (Table 1). These data suggest a model wherein water-mediated $\text{CH}\cdots\text{O}$ hydrogen bonding between the AdoMet sulfonium cation and acidic residues within the active site of a methyltransferase may serve to enhance substrate recognition. In contrast, water-bridged interactions involving amino acids with neutral polar side chains would potentially form weaker hydrogen bonds that do not contribute to selective AdoMet recognition, consistent with the effect of the glutamate to glutamine substitutions in MetH (Table 1). These findings merit further investigation into how acidic residues may facilitate AdoMet recognition in other methyltransferases.

These results also offer new insights into how the AdoMet/AdoHcy ratio may govern MetH activity in cells. The *E. coli* MetH reactivation domain displayed a 15-fold higher affinity for AdoMet than AdoHcy (Table 1). This difference in selectivity is achieved in part by water-

mediated hydrogen bonding between AdoMet and Glu1097 and Glu1128 in the enzyme. In mammalian MetH, the residue corresponding to Glu1128 in the *E. coli* enzyme is substituted by a leucine.²⁹ Based on the effects of the *E. coli* MetH E1128Q mutant (Table 1), the leucine substitution would presumably diminish its ability to discriminate between AdoMet and AdoHcy, rendering it more susceptible to product inhibition. Mammalian studies investigating AdoMet and AdoHcy concentrations have reported AdoMet/AdoHcy ratios ranging between two to eleven, depending on the tissue type.^{30, 31} Metabolic changes that elevate the concentration of AdoHcy and lower the AdoMet/AdoHcy ratio would potentially inhibit the MetH reactivation domain, thus resulting in diminished reactivation of the enzyme with concomitant alterations in the cellular methyl cycle.

Prior studies of a disulfide-stabilized C-terminal construct of *E. coli* MetH comprising the cobalamin-binding and reactivation domains have revealed that Glu1097 also has a catalytic role in the reactivation cycle.^{8, 9} The structure of this C-terminal MetH construct bound to cobalamin and AdoHcy illustrates that the side chains of the Glu1097 and Tyr1139 form hydrogen bonds to a water molecule coordinated to the Co ion in the cofactor. These interactions stabilize the 4-coordinate state of Co(II)Cbl, promoting the one electron reduction of Co(II)Cbl to Co(I)Cbl. Structures of the C-terminal construct determined in the absence and presence of AdoHcy indicate that the side chain of Glu1097 changes conformation to engage in hydrogen bonding with the Co-coordinated water molecule when AdoHcy is bound, which would also presumably occur when AdoMet is present. Thus, Glu1097, which is invariant in MetH, may serve two functions in the enzyme: 1) to enhance AdoMet binding affinity through water-mediated CH \cdots O hydrogen bonding and 2) to modulate the reduction potential of Co(II)Cbl by hydrogen bonding to the Co-bound water molecule.

1
2
3 Finally, our results have important ramifications with respect to the development of
4 AdoMet analogs as competitive inhibitors of methyltransferases. Several of these inhibitors
5 utilize sinefungin, a natural product pan-methyltransferase inhibitor, as a scaffold given its
6 isostericity with AdoMet.³²⁻³⁶ Given that sinefungin recognizes the MetH reactivation domain
7 with affinity comparable to AdoMet (Table 1), analogs derived from it may also bind to the
8 enzyme, particularly due to the solvent exposure of the substrate binding cleft that can
9 accommodate chemical derivatizations of the inhibitor (Figure S2). Sinefungin has been reported
10 to cause severe nephrotoxicity in mammalian models of cryptosporidiosis and
11 trypanosomiasis.^{37, 38} It is conceivable that this toxicity is due not only to widespread inhibition
12 of AdoMet-dependent methyltransferases, but also to abrogation of MetH reactivation, disrupting
13 methionine biosynthesis and the cellular methyl cycle. In light of these findings, it would be
14 advisable that future efforts to devise AdoMet-based inhibitors of methyltransferases evaluate
15 whether these compounds inhibit the reactivation domain of MetH to circumvent off-target
16 effects of these molecules *in vivo*.
17
18
19
20
21
22
23
24
25
26
27
28
29
30
31
32
33
34
35
36
37
38
39
40
41
42
43
44
45
46
47
48
49
50
51
52
53
54
55
56
57
58
59
60

ASSOCIATED CONTENT

Supporting Information

A table reporting the crystallographic and refinement statistics, and figures illustrating the ligand
omit maps, AdoMet binding sites of MetH and SET7/9, ITC data, and models used for the QM
calculations.

Structure Accession Codes

1
2
3 Coordinates and structure factors for the complexes of MetH•AdoMet (6BM5), MetH•AdoHcy
4
5 (6BM6), and MetH•sinefungin (6BDY) have been deposited into the RCSB PDB.
6
7
8
9
10
11

12 Acknowledgments 13

14
15 We thank M. Koutmos for providing the cDNA encoding the *E. coli* MetH reactivation domain
16 and S. Horowitz for the reading the manuscript and furnishing insightful comments and
17 feedback. This work was supported by NSF grant CHE-1508492 to R. Trievle. This research
18 used resources of the Advanced Photon Source, a U.S. Department of Energy (DOE) Office of
19 Science User Facility operated for the DOE Office of Science by Argonne National Laboratory
20 under Contract No. DE-AC02-06CH11357. Use of the LS-CAT Sector 21 was supported by the
21 Michigan Economic Development Corporation and the Michigan Technology Tri-Corridor
22 (Grant 085P1000817).
23
24
25
26
27
28
29
30
31

32 REFERENCES 33 34 35

36
37 [1] Matthews, R. G., Koutmos, M., and Datta, S. (2008) Cobalamin-dependent and cobamide-
38 dependent methyltransferases, *Curr Opin Struct Biol* 18, 658-666.
39
40 [2] Ludwig, M. L., and Matthews, R. G. (1997) Structure-based perspectives on B12-dependent
41 enzymes, *Annu Rev Biochem* 66, 269-313.
42
43 [3] Banerjee, R. V., and Matthews, R. G. (1990) Cobalamin-dependent methionine synthase,
44 *Faseb J* 4, 1450-1459.
45
46 [4] Drummond, J. T., Huang, S., Blumenthal, R. M., and Matthews, R. G. (1993) Assignment of
47 enzymatic function to specific protein regions of cobalamin-dependent methionine
48 synthase from *Escherichia coli*, *Biochemistry* 32, 9290-9295.
49
50 [5] Dixon, M. M., Huang, S., Matthews, R. G., and Ludwig, M. (1996) The structure of the C-
51 terminal domain of methionine synthase: Presenting S-adenosylmethionine for reductive
52 methylation of B-12, *Structure* 4, 1263-1275.
53
54 [6] Schubert, H. L., Blumenthal, R. M., and Cheng, X. (2003) Many paths to methyltransfer: a
55 chronicle of convergence, *Trends Biochem Sci* 28, 329-335.
56
57
58
59
60

[7] Bandarian, V., Patridge, K. A., Lennon, B. W., Huddler, D. P., Matthews, R. G., and Ludwig, M. L. (2002) Domain alternation switches B(12)-dependent methionine synthase to the activation conformation, *Nat Struct Biol* 9, 53-56.

[8] Datta, S., Koutmos, M., Patridge, K. A., Ludwig, M. L., and Matthews, R. G. (2008) A disulfide-stabilized conformer of methionine synthase reveals an unexpected role for the histidine ligand of the cobalamin cofactor, *Proc Natl Acad Sci U S A* 105, 4115-4120.

[9] Koutmos, M., Datta, S., Patridge, K. A., Smith, J. L., and Matthews, R. G. (2009) Insights into the reactivation of cobalamin-dependent methionine synthase, *Proc Natl Acad Sci U S A* 106, 18527-18532.

[10] Horowitz, S., Dirk, L. M., Yesselman, J. D., Nimtz, J. S., Adhikari, U., Mehl, R. A., Scheiner, S., Houtz, R. L., Al-Hashimi, H. M., and Trievle, R. C. (2013) Conservation and functional importance of carbon-oxygen hydrogen bonding in AdoMet-dependent methyltransferases, *J Am Chem Soc* 135, 15536-15548.

[11] Horowitz, S., Yesselman, J. D., Al-Hashimi, H. M., and Trievle, R. C. (2011) Direct evidence for methyl group coordination by carbon-oxygen hydrogen bonds in the lysine methyltransferase SET7/9, *J Biol Chem* 286, 18658-18663.

[12] Fick, R. J., Kroner, G. M., Nepal, B., Magnani, R., Horowitz, S., Houtz, R. L., Scheiner, S., and Trievle, R. C. (2016) Sulfur-Oxygen Chalcogen Bonding Mediates AdoMet Recognition in the Lysine Methyltransferase SET7/9, *ACS Chem Biol* 11, 748-754.

[13] Otwinowski, Z., and Minor, W. (1997) Processing of X-ray diffraction data collected in oscillation mode, *Methods Enzymol* 276, 307-326.

[14] Mccoy, A. J., Grosse-Kunstleve, R. W., Adams, P. D., Winn, M. D., Storoni, L. C., and Read, R. J. (2007) Phaser crystallographic software, *J Appl Crystallogr* 40, 658-674.

[15] Emsley, P., and Cowtan, K. (2004) Coot: model-building tools for molecular graphics, *Acta Crystallogr D* 60, 2126-2132.

[16] Emsley, P., Lohkamp, B., Scott, W. G., and Cowtan, K. (2010) Features and development of Coot, *Acta Crystallogr D* 66, 486-501.

[17] Adams, P. D., Afonine, P. V., Bunkoczi, G., Chen, V. B., Davis, I. W., Echols, N., Headd, J. J., Hung, L. W., Kapral, G. J., Grosse-Kunstleve, R. W., McCoy, A. J., Moriarty, N. W., Oeffner, R., Read, R. J., Richardson, D. C., Richardson, J. S., Terwilliger, T. C., and Zwart, P. H. (2010) PHENIX: a comprehensive Python-based system for macromolecular structure solution, *Acta Crystallogr D Biol Crystallogr* 66, 213-221.

[18] Baker, N. A., Sept, D., Joseph, S., Holst, M. J., and McCammon, J. A. (2001) Electrostatics of nanosystems: application to microtubules and the ribosome, *Proc Natl Acad Sci U S A* 98, 10037-10041.

[19] Goddard, T. G., Kneller D.G. SPARKY 3, University of California, San Francisco.

[20] Delaglio, F., Grzesiek, S., Vuister, G. W., Zhu, G., Pfeifer, J., and Bax, A. (1995) NMRPipe - a Multidimensional Spectral Processing System Based on Unix Pipes, *J Biomol Nmr* 6, 277-293.

[21] Frisch, M. J., Trucks, G. W., Schlegel, H. B., Scuseria, G. E., Robb, M. A., Cheeseman, J. R., Scalmani, G., Barone, V., Mennucci, B., Petersson, G. A., Nakatsuji, H., Caricato, M., Li, X., Hratchian, H. P., Izmaylov, A. F., Bloino, J., Zheng, G., Sonnenberg, J. L., Hada, M., Ehara, M., Toyota, K., Fukuda, R., Hasegawa, J., Ishida, M., Nakajima, T., Honda, Y., Kitao, O., Nakai, H., Vreven, T., Montgomery, J., J. A., Peralta, J. E., Ogliaro, F., Bearpark, M., Heyd, J. J., Brothers, E., Kudin, K. N., Staroverov, V. N., Kobayashi, R., Normand, J., Raghavachari, K., Rendell, A., Burant, J. C., Iyengar, S. S., Tomasi, J.,

1
2
3 Cossi, M., Rega, N., Millam, J. M., Klene, M., Knox, J. E., Cross, J. B., Bakken, V.,
4 Adamo, C., Jaramillo, J., Gomperts, R., Stratmann, R. E., Yazyev, O., Austin, A. J.,
5 Cammi, R., Pomelli, C., Ochterski, J. W., Martin, R. L., Morokuma, K., Zakrzewski, V.
6 G., Voth, G. A., Salvador, P., Dannenberg, J. J., Dapprich, S., Daniels, A. D., Farkas, O.,
7 Foresman, J. B., Ortiz, J. V., Cioslowski, J., and Fox, D. J. (2009) Gaussian 09, Revision
8 B.01 ed., Wallingford, CT.
9
10 [22] Zhao, Y., and Truhlar, D. G. (2008) The M06 suite of density functionals for main group
11 thermochemistry, thermochemical kinetics, noncovalent interactions, excited states, and
12 transition elements: two new functionals and systematic testing of four M06-class
13 functionals and 12 other functionals, *Theor. Chem. Acc.* 120, 215-241.
14
15 [23] Barone, V., and Cossi, M. (1998) Quantum calculation of molecular energies and energy
16 gradients in solution by a conductor solvent model, *J. Phys. Chem. A* 102, 1995-2001.
17
18 [24] Adhikari, U., and Scheiner, S. (2013) Magnitude and mechanism of charge enhancement of
19 CH $\bullet\bullet$ O hydrogen bonds, *J Phys Chem A* 117, 10551-10562.
20
21 [25] Seeger, K., Lein, S., Reuter, G., and Berger, S. (2005) Saturation transfer difference
22 measurements with SU(VAR)3-9 and S-adenosyl-L-methionine, *Biochemistry* 44, 6208-
23 6213.
24
25 [26] Schanda, P., Kupce, E., and Brutscher, B. (2005) SOFAST-HMQC experiments for
26 recording two-dimensional heteronuclear correlation spectra of proteins within a few
27 seconds, *J Biomol Nmr* 33, 199-211.
28
29 [27] Horowitz, S., Adhikari, U., Dirk, L. M., Del Rizzo, P. A., Mehl, R. A., Houtz, R. L., Al-
30 Hashimi, H. M., Scheiner, S., and Trievle, R. C. (2014) Manipulating unconventional
31 CH-based hydrogen bonding in a methyltransferase via noncanonical amino acid
32 mutagenesis, *ACS Chem Biol* 9, 1692-1697.
33
34 [28] Couture, J. F., Hauk, G., Thompson, M. J., Blackburn, G. M., and Trievle, R. C. (2006)
35 Catalytic roles for carbon-oxygen hydrogen bonding in SET domain lysine
36 methyltransferases, *J Biol Chem* 281, 19280-19287.
37
38 [29] Wolthers, K. R., Toogood, H. S., Jowitt, T. A., Marshall, K. R., Leys, D., and Scrutton, N.
39 S. (2007) Crystal structure and solution characterization of the activation domain of
40 human methionine synthase, *FEBS J* 274, 738-750.
41
42 [30] Caudill, M. A., Wang, J. C., Melnyk, S., Pogribny, I. P., Jernigan, S., Collins, M. D.,
43 Santos-Guzman, J., Swendseid, M. E., Cogger, E. A., and James, S. J. (2001)
44 Intracellular S-adenosylhomocysteine concentrations predict global DNA
45 hypomethylation in tissues of methyl-deficient cystathione beta-synthase heterozygous
46 mice, *J Nutr* 131, 2811-2818.
47
48 [31] Smith, D. E., Hornstra, J. M., Kok, R. M., Blom, H. J., and Smulders, Y. M. (2013) Folic
49 acid supplementation does not reduce intracellular homocysteine, and may disturb
50 intracellular one-carbon metabolism, *Clin Chem Lab Med* 51, 1643-1650.
51
52 [32] Cai, X. C., Kapilashrami, K., and Luo, M. (2016) Synthesis and Assays of Inhibitors of
53 Methyltransferases, *Methods Enzymol* 574, 245-308.
54
55 [33] Tisi, D., Chiarparrin, E., Tamanini, E., Pathuri, P., Coyle, J. E., Hold, A., Holding, F. P.,
56 Amin, N., Martin, A. C., Rich, S. J., Berdini, V., Yon, J., Acklam, P., Burke, R., Drouin,
57 L., Harmer, J. E., Jeganathan, F., van Montfort, R. L., Newbatt, Y., Tortorici, M.,
58 Westlake, M., Wood, A., Hoelder, S., and Heightman, T. D. (2016) Structure of the
59 Epigenetic Oncogene MMSET and Inhibition by N-Alkyl Sinefungin Derivatives, *ACS
60 Chem Biol* 11, 3093-3105.

1

2

3 [34] Devkota, K., Lohse, B., Liu, Q., Wang, M. W., Staerk, D., Berthelsen, J., and Clausen, R. P.
4 (2014) Analogues of the Natural Product Sinefungin as Inhibitors of EHMT1 and
5 EHMT2, *ACS Med Chem Lett* 5, 293-297.

6

7 [35] Liu, Q., Cai, X., Yang, D., Chen, Y., Wang, Y., Shao, L., and Wang, M. W. (2017)
8 Cycloalkane analogues of sinefungin as EHMT1/2 inhibitors, *Bioorg Med Chem* 25,
9 4579-4594.

10

11 [36] Zheng, W., Ibanez, G., Wu, H., Blum, G., Zeng, H., Dong, A., Li, F., Hajian, T., Allali-
12 Hassani, A., Amaya, M. F., Siarheyeva, A., Yu, W., Brown, P. J., Schapira, M., Vedadi,
13 M., Min, J., and Luo, M. (2012) Sinefungin derivatives as inhibitors and structure probes
14 of protein lysine methyltransferase SETD2, *J Am Chem Soc* 134, 18004-18014.

15

16 [37] Zweygarth, E., Schillinger, D., Kaufmann, W., and Rottcher, D. (1986) Evaluation of
17 sinefungin for the treatment of Trypanosoma (Nannomonas) congolense infections in
18 goats, *Trop Med Parasitol* 37, 255-257.

19

20 [38] Kalimouttou, S., Skiba, M., Bon, P., Dechelotte, P., Arnaud, P., and Lahiani-Skiba, M.
21 (2009) Sinefungin-PLGA nanoparticles: drug loading, characterization, in vitro drug
22 release and in vivo studies, *J Nanosci Nanotechnol* 9, 150-158.

23

24

25

26

27

28

29

30

31

32

33

34

35

36

37

38

39

40

41

42

43

44

45

46

47

48

49

50

51

52

53

54

55

56

57

58

59

60